RESEARCH ARTICLE

Integrated Microfluidic Card with TaqMan Probes and High-Resolution Melt Analysis To Detect Tuberculosis Drug Resistance Mutations across 10 Genes

Suporn Pholwat,[a] Jie Liu,[a] Suzanne Stroup,[a] Jean Gratz,[a] Sayera Banu,[b] S. M. Mazidur Rahman,[b] Sara Sabrina Ferdous,[b] Suporn Foongladda,[c] Duangjai Boonlert,[c] Oleg Ogarkov,[d,e] Svetlana Zhdanova,[d] Gibson Kibiki,[f] Scott Heysell,[a] Eric Houpt[a]

Division of Infectious Diseases and International Health, Department of Medicine, University of Virginia, Charlottesville, Virginia, USA[a]; International Center for Diarrheal Diseases and Research, Dhaka, Bangladesh[b]; Department of Microbiology, Faculty of Medicine, Siriraj Hospital, Mahidol University, Bangkok, Thailand[c]; Scientific Center of Family Health and Reproductive Problems, Siberian Branch, Russian Academy of Medical Sciences, Irkutsk, Russia[d]; Regional TB Prevention Dispensary, Irkutsk, Russia[e]; Kilimanjaro Clinical Research Institute, Moshi, Tanzania[f]

ABSTRACT **Genotypic methods for drug susceptibility testing of *Mycobacterium tuberculosis* are desirable to speed the diagnosis and proper therapy of tuberculosis (TB). However, the numbers of genes and polymorphisms implicated in resistance have proliferated, challenging diagnostic design. We developed a microfluidic TaqMan array card (TAC) that utilizes both sequence-specific probes and high-resolution melt analysis (HRM), providing two layers of detection of mutations. Twenty-seven primer pairs and 40 probes were designed to interrogate 3,200 base pairs of critical regions of the *inhA*, *katG*, *rpoB*, *embB*, *rpsL*, *rrs*, *eis*, *gyrA*, *gyrB*, and *pncA* genes. The method was evaluated on 230 clinical *M. tuberculosis* isolates from around the world, and it yielded 96.1% accuracy (2,431/2,530) in comparison to that of Sanger sequencing and 87% accuracy in comparison to that of the slow culture-based susceptibility testing. This TAC-HRM method integrates assays for 10 genes to yield fast, comprehensive, and accurate drug susceptibility results for the 9 major antibiotics used to treat TB and could be deployed to improve treatment outcomes.**

IMPORTANCE **Multidrug-resistant tuberculosis threatens global tuberculosis control efforts. Optimal therapy utilizes susceptibility test results to guide individualized treatment regimens; however, the susceptibility testing methods in use are technically difficult and slow. We developed an integrated TaqMan array card method with high-resolution melt analysis that interrogates 10 genes to yield a fast, comprehensive, and accurate drug susceptibility result for the 9 major antituberculosis antibiotics.**

Received 7 November 2014 **Accepted** 8 January 2015 **Published** 24 February 2015

Citation Pholwat S, Liu J, Stroup S, Gratz J, Banu S, Rahman SMM, Ferdous SS, Foongladda S, Boonlert D, Ogarkov O, Zhdanova S, Kibiki G, Heysell S, Houpt E. 2015. Integrated microfluidic card with TaqMan probes and high-resolution melt analysis to detect tuberculosis drug resistance mutations across 10 genes. mBio 6(2):e02273-14. doi:10.1128/mBio.02273-14.

Invited Editor Melissa B. Miller, UNC School of Medicine **Editor** Peter Gilligan, UNC Health Care System

Address correspondence to Eric Houpt, erh6k@virginia.edu.

Multidrug-resistant tuberculosis (MDR-TB), defined as resistance of the *Mycobacterium tuberculosis* to isoniazid and rifampin, occurred in an estimated 440,000 individuals worldwide in 2008 (1). Diagnostic assays for drug-resistant tuberculosis are a key element in MDR-TB control, and genotypic drug resistance testing to detect rifampin resistance has become widespread. Once it is detected, however, most countries employ a standardized treatment regimen, despite the fact that better outcomes are associated with individualized drug susceptibility testing (2, 3), because obtaining a complete antibiotic susceptibility profile is resource intensive and requires several culture-based methodologies and significant technical capacity. Furthermore, nonsusceptibility of the pathogen to a number of drugs in the standardized treatment regimens has been associated with the amplification of acquired drug resistance, including the development of extensively drug-resistant (XDR)-TB, while patients are on MDR-TB therapy (4). We sought to develop a single integrated genotypic susceptibility testing method that can provide an accurate result, compared with that of culture, for the most important drugs used to treat MDR-TB, which could significantly improve outcomes and curb the amplification of drug resistance.

There are several drugs used to treat drug-resistant TB, and for each, drug resistance correlates to differing degrees with several mutations in one or more genes. WHO-approved diagnostic assays include the GeneXpert MTB/RIF, INNO-LiPA Rif TB, and GenoType MTBDRplus, which interrogate regions of *rpoB* to yield information on rifampin resistance, and some assays include *inhA* and *katG* for information on isoniazid. The GenoType MTBDRsl adds regions of *embB*, *rrs*, and *gyrA* to yield partial information on ethambutol, aminoglycosides, and quinolones, respectively (5–8). Several important drugs for MDR treatment, such as pyrazinamide and kanamycin, are not currently assayed with these methods, and quinolone coverage is limited because of the lack of *gyrB* (9). Since additional genes are desirable and new resistance-associated mutations are steadily being identified, the challenges of molecular diagnostic design and interpretation of

results has increased. Sanger sequencing is highly valuable in this regard (10), because it provides precise sequence information that can be compared against resistance databases. However, like most of the other technologies mentioned, it requires multiple steps and postamplification manipulations and has a limited ability to detect mixed populations (11). We therefore sought to create a single, comprehensive, easy-to-perform genotypic method.

The TaqMan array card (TAC) is a customizable 384-well microfluidic real-time PCR system that compartmentalizes each sample into 48 different PCRs simultaneously and has been applied for the detection of multiple respiratory or enteric pathogens (12, 13). In this work, we sourced the largest *M. tuberculosis* sequence databases to identify the most prominent drug resistance-associated mutations in key regions of 10 genes and design mutation-specific probes. Additionally, to cover rare or unknown mutations in these areas, we also incorporated a high-resolution melt analysis (HRM) to evaluate whether any mutation was present in these regions. This HRM technique is particularly advantageous for genes like *pncA*, where single resistance-associated mutations are dispersed throughout a large region (14–19), and yet the method has never been attempted in microliter volumes. Ultimately, we designed 27 amplicons, 40 mutation-specific probes, and HRM to simultaneously and accurately detect in one sample the TB drug resistance-associated mutations in *inhA* and *katG* (isoniazid), *rpoB* (rifampin), *embB* (ethambutol), *rpsL* (streptomycin), *rrs* (streptomycin, amikacin, kanamycin, and capreomycin), *eis* (kanamycin), *gyrA* and *gyrB* (ofloxacin and moxifloxacin), and *pncA* (pyrazinamide).

RESULTS

Identification of key mutations associated with TB drug resistance and probe design. We first scrutinized the published literature for the key resistance-associated mutations in the above-mentioned genes using the large databases of Campbell et al., Rodwell et al., and the TB Drug Resistance Mutation Database (Table S1 in the supplemental material) (10, 20, 21). We arrived at 38 specific resistance probes that we predicted would detect ~90% of the *rpoB* mutations that are found in rifampin-resistant tuberculosis, ~90% of the *inhA* and *katG* mutations that are found in isoniazid-resistant tuberculosis, ~70% of the *embB* mutations found in ethambutol-resistant tuberculosis, ~70% of the *rpsL* and *rrs* mutations found in streptomycin-resistant tuberculosis, ~80% of the *rrs* and *eis* mutations found in amikacin- or kanamycin-resistant tuberculosis, and ~75% of the *gyrA* and *gyrB* mutations found in quinolone-resistant tuberculosis. We also included one *pncA* probe specific to the His57Asp (CAC→GAC) of *Mycobacterium bovis* and one probe for the common *pncA* silent mutation Ser65Ser (TCC→TCT). Primer/probe sequences are listed in Table S2. Stringent specificity of probes was required for this application, and many redesigns were required (data not shown). As an illustration of the results, the *rrs* (amplicon 3) primer/probe set detected a mutant isolate using the *rrs*-A(1401)G-specific probe (detects the A-to-G change at position 1401 encoded by *rrs*), while the wild-type, drug-susceptible laboratory strain *M. tuberculosis* H37Rv was negative (Fig. 1A).

High-resolution melt analysis in the microfluidic card format. To gain additional coverage of the less frequent (e.g., 2 to 10%) resistance-associated mutations, we designed 27 amplicons to adequately cover the necessary gene segments. These included one region for *inhA*, *katG*, *eis*, and *gyrA*, two for *rpoB* and *rpsL*, three for *embB* and *gyrB*, four regions for *rrs* (2 regions for streptomycin resistance and another 2 regions for amikacin, kanamycin, and capreomycin resistance), and nine for *pncA* (Table S2 in the supplemental material). The HRM assay had not been performed within such a small volume (1 μl), and we constructed an internal control plasmid with one defined mutant in every amplicon region to be included in every card as a positive control, along with *M. tuberculosis* H37Rv as a negative control. For the melt curve analysis, leftward variation indicates a lower melt temperature (e.g., C→A, C→T, G→A, G→T) and rightward variation a higher melt temperature (e.g., A→C, T→C, A→G, T→G) compared with the melt curves of the *M. tuberculosis* H37Rv wild-type control. The difference graph uses the melt data but plots the negative first derivative ($-dF/dt$) on the y axis, with positive curves indicating higher melt temperatures and negative curves indicating lower melt temperatures. Both the mutant isolate and H37Rv were amplified, as indicated by the nonspecific dye SYTO9 (Fig. 1B); however, the HRM result reinforced the probe result for mutant/variant samples (Fig. 1C and D). Similarly, the *gyrB* (amplicon 2) primer/probe set demonstrated the benefit of combining the use of probes with HRM, since the specific probe (Fig. 1E) detected the important Asp461His (GAC→CAC) transversion, while HRM would not (Fig. 1F, G, and H). However, rare mutations, so long as they were not transversions (Asp461Ala and Asp461Asn, for instance), would be categorized as variant by HRM. Other combinations of probe-HRM results for specific mutations are shown for *katG*, *rpoB* (amplicon 1), *embB* (amplicon 3), *rpsL* (amplicon 1), *rrs* (amplicon 2), *rrs* (amplicon 4), and *gyrA* (Fig. S1). The *pncA* gene can carry resistance-associated mutations dispersed upstream and throughout its 561-base pair open reading frame. Therefore, resistance probes were not feasible with this platform and, apart from the above-mentioned His57Asp (CAC→GAC) of *M. bovis* and the Ser65Ser silent mutation probe, we relied on melt curve analysis of 9 overlapping amplicons, whereby a variant in any amplicon is inferred to be a mutation (Fig. S2A and B). HRM examples for all of the other genes, *inhA*, *katG*, *rpoB*, *embB*, *rpsL*, *rrs*, *eis*, *gyrA*, and *gyrB*, are shown in Fig. S3.

Evaluation using clinical isolates. The final TAC card was thus configured (Fig. 2) and was evaluated using 110 Sanger-sequenced clinical TB strains. The layout shows, for example, that *rpoB* is amplified in 9 wells, using two amplicons. Amplicon 1 is amplified in 4 wells that include distinct resistance probes (511Pro, 513Leu, 513Glu, and 516Val), while amplicon 2 is amplified in 5 wells with 6 distinct probes (526Tyr, 526Asp, 526Leu, 533Pro, and 531Leu/531Trp in multiplex). To evaluate the reliability of the HRM software determinations, the difference values of amplicons versus wild-type control of the 110 isolates were plotted (Fig. 3; Fig. S4 in the supplemental material). Based on receiver operating characteristic (ROC) analysis, difference value cutoffs of between 6 and 10 were optimal to discriminate susceptible and resistant isolates, where lower numbers would be categorized as wild-type and higher numbers would be categorized as variant. A difference value of 9 was optimal for the majority of amplicons (13/26). A benefit of the TAC layout is that most regions are amplified and subjected to HRM in multiple wells, and thus, difference values can be averaged; we observed low standard deviations (Fig. 3). As would be expected, however, transversion mutations were not detected by HRM.

Using these difference value cutoffs, we then prospectively analyzed another 120 clinical isolates (total number analyzed, 230)

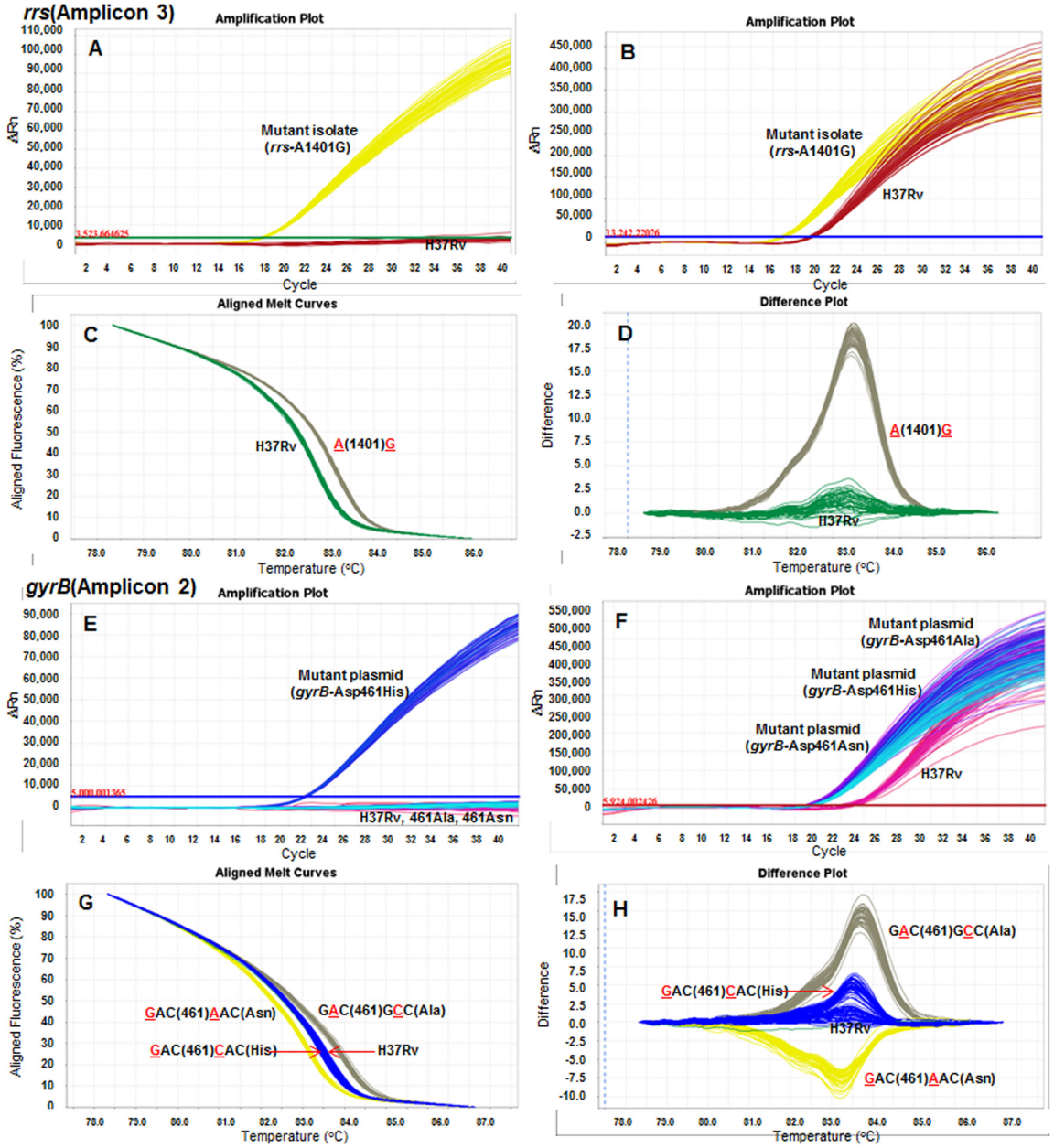

FIG 1 TAC-HRM of *rrs* (amplicon 3) and *gyrB* (amplicon 2) gene segments. Singleplex PCR mixtures with primers and probes were loaded into empty microfluidic cards (1 sample per port, yielding 48 reaction mixtures per sample). Results are shown for probe-based detection (A and E), for amplification with SYTO9 (B and F), and for melt curve and difference curve analysis (C and D, G and H). The aligned melt curves show melt temperature shifts versus those for the *M. tuberculosis* H37Rv wild-type control based on nucleotide changes (leftward variation indicates a lower melt temperature and rightward variation a higher melt temperature). The difference plot uses the same data but plots the negative first derivative ($-dF/dt$) on the *y* axis. The HRM software automatically labels samples that are variants from the wild-type control with a different color. Underlining indicates nucleotides that changed. The *rrs* (amplicon 3) primer/probe results show the amplification curve obtained with the *rrs*-A(1401)G-specific probe for a mutant isolate, while the results for *M. tuberculosis* H37Rv were negative. Both the mutant isolate and H37Rv amplified with the primers using SYTO9, and the HRM result reinforced the probe result as being a mutant/variant sample. The *gyrB* (amplicon 2) primer/probe results demonstrated the benefit of combining the probe with HRM, since the specific probe (E) detected the Asp461His (GAC→CAC) transversion, while HRM would not (F, G, and H); however, HRM detected the rare mutations Asp461Ala and Asp461Asn.

and compared the performance of TAC-HRM versus Sanger sequencing of the same regions (Table 1). For this analysis, TAC-HRM was considered variant either if the probe yielded detection or a variant was called by HRM, and a Sanger sequencing gold standard was used that included not only detection of mutations but, also, detection of mutations associated with resistance, as described in Table S1 in the supplemental material. The overall accuracy versus this Sanger-identified resistance-associated mutation standard was 96.1% (2,431/2,530), and the accuracy exceeded 95% for all genes except *pncA* (81%), which was partly explained by transversions (Table 1). Next, we compared the performance of TAC-HRM to the phenotypic drug susceptibility results for these

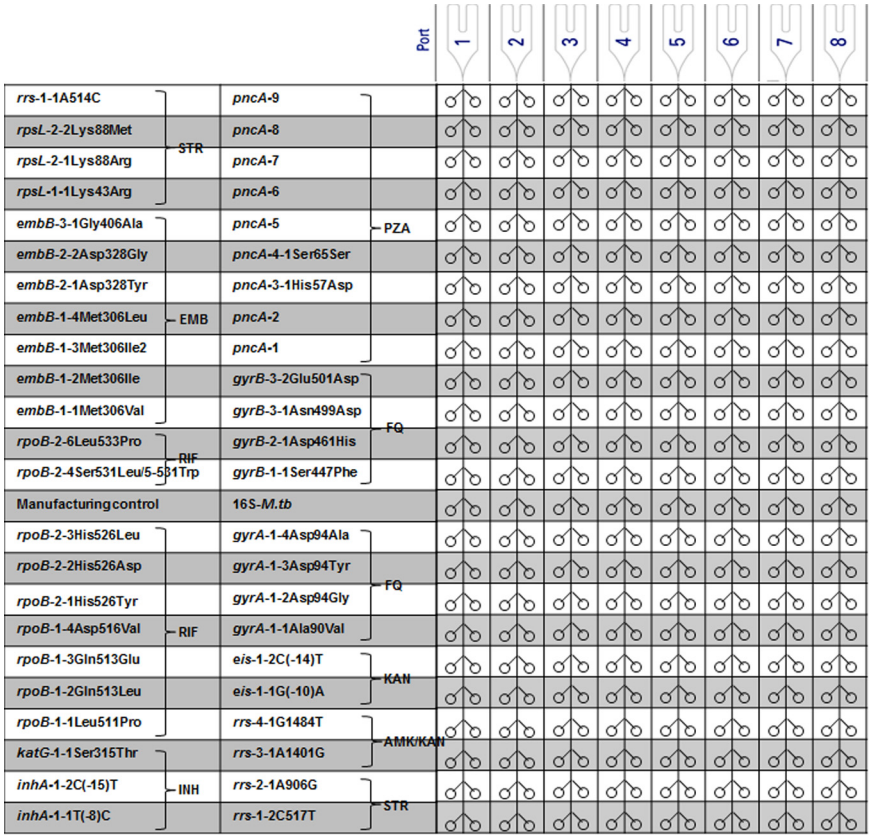

FIG 2 TB drug resistance TAC-HRM card. Each well was configured as shown on the basis of gene, amplicon, and mutation-specific probe, grouped according to drug susceptibility information for STR (streptomycin), EMB (ethambutol), RIF (rifampin), INH (isoniazid), PZA (pyrazinamide), FQ (fluoroquinolones), KAN (kanamycin), and AMK (amikacin).

isolates (Table 2). Different phenotypic methods were used, as indicated in Materials and Methods, and if multiple methods were used, isolates with discordant phenotypic results were excluded. The accuracy of TAC-HRM versus phenotypic drug susceptibility testing averaged 87%, ranging from 72 to 94% for the 7 drugs. Sanger sequencing versus phenotypic results are shown for comparison and revealed similar levels of accuracy (average, 90%, and range, 74 to 95%). We used Sanger sequencing to adjudicate the 175 discrepancies for TAC-HRM versus phenotypic testing and found that most (73%) were supported by the Sanger result.

DISCUSSION

This work details the design and development of a comprehensive microfluidic card that targets the most common TB drug resistance-associated mutations with TaqMan probes and, importantly, utilizes high-resolution melt analysis (HRM) to cover gaps missed by the probes. As was predicted by the synthesis of information from TB drug resistance mutation databases, this assay and its choice of mutations yielded a result that was on average 87% accurate in comparison to the culture-based drug susceptibility results, ranging from 72 to 94% for the different drugs. Shortcomings were mostly due to true genotypic-phenotypic discordance and not assay failure, as evidenced by the rigorous comparison against the Sanger sequencing result for the same genes. We remain advocates of Sanger sequencing, since it yields precise genotypic information and can also afford resistance interpretation. However, it does have limited detection of heteroresistance, requires days for amplification and postamplification processing in specialized laboratories, and in contrast to real-time PCR, simply is not readily available in the representative areas of TB endemicity where we work (Thailand, Bangladesh, Tanzania, and Russian Federation) (11). Next-generation-sequencing technologies are being developed, but presently, the number of steps and bioinformatic requirements are cumbersome for field use. Therefore, the use of a closed-system, rapid, comprehensive assay like the TAC-HRM offers a considerable advance. In particular, we have previously demonstrated how well the TAC platform works in laboratories in these countries, since the cards are stable at ambient temperature and all reagents are enclosed (22).

The assay provides two independent layers of resolution for mutations, both through resistance-specific probes and through HRM, which can indicate whether a region is non-wild type. Two layers are useful because neither is perfect (i.e., we encountered instances where probes detected mutations while HRM did not, and vice versa). The strategy of detecting non-wild-type regions is a common one and is, for example, the basis of the rifampin resistance result from the GeneXpert MTB/RIF (Cepheid, United States). However, careful design is required to avoid regions with known silent mutations that would result in false resistance being called; alternatively, nonresistance-specific probes can be included (e.g., as we have done with *pncA* Ser65Ser) to negate false

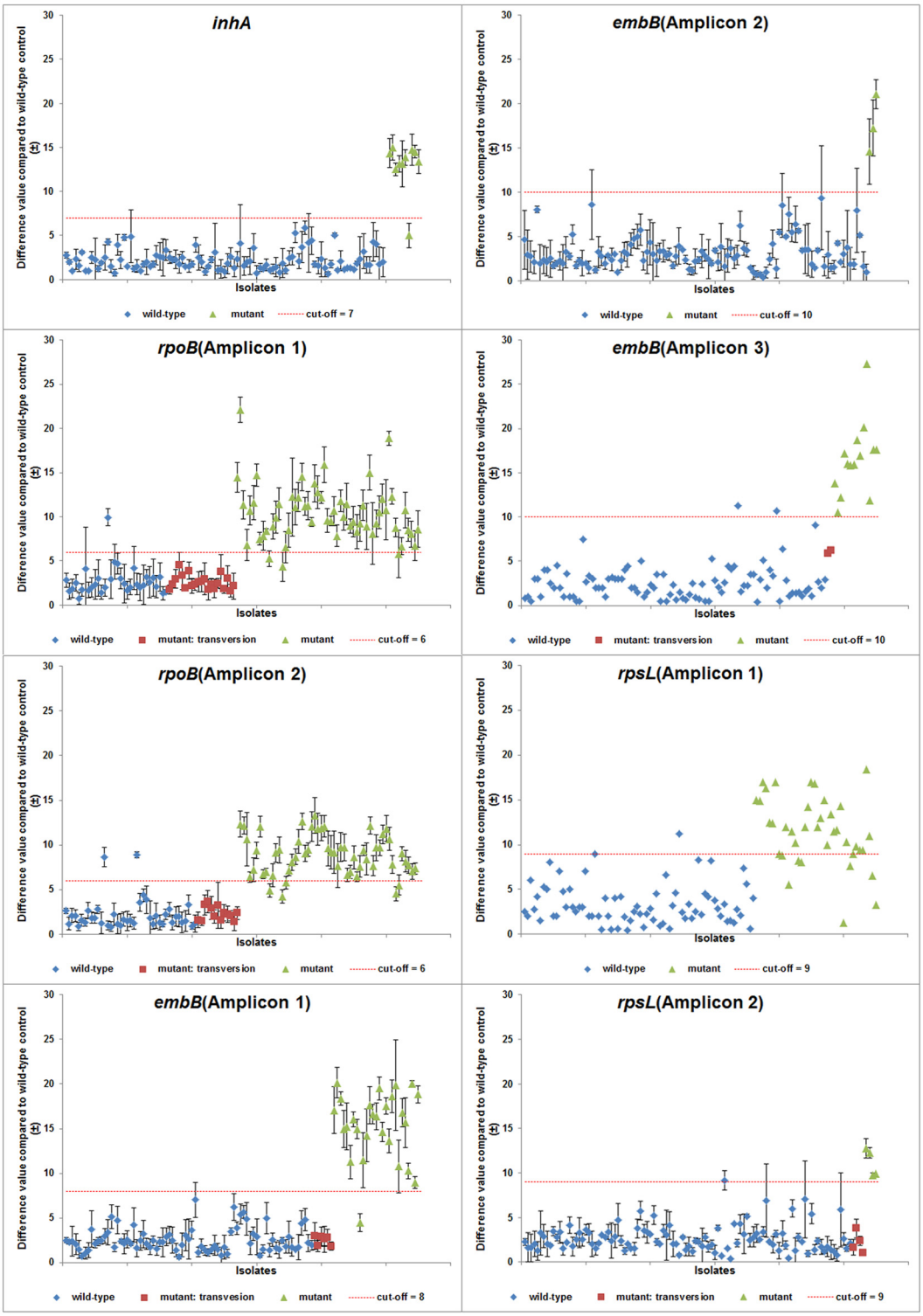

FIG 3 Scatterplot of difference values of the 110 Sanger-sequenced isolates against wild type for *inhA*, *rpoB*, *embB*, and *rpsL*. For replicate amplicons, the difference plots are shown as means ± standard deviations. Receiver operating curves identified cutoffs for difference values that optimized variant/nonvariant categorization by TAC-HRM against Sanger sequencing.

variant calls. Another shortcoming of HRM is that transversions may be missed; however, this was overcome with specific probes and was otherwise rarely a problem; for instance, it only occurred in 2 of 14 of the *pncA* nonvariant isolates.

There were limitations to this work. The TAC platform still requires an expensive real-time PCR platform, and currently, the HRM software requires manual reading of the difference values. Additionally, the HRM requires high-quality DNA from purified

TABLE 1 Performance of TaqMan array card high-resolution melt compared to sequencing

Target gene	TAC-HRM result	No. with resistance-associated mutation found or not found by sequencing		% sensitivity	% specificity
		Found	Not found		
inhA	Variant	28	1	100	100
	Nonvariant	0	201		
katG	Variant	157	2	100	97
	Nonvariant	0	71		
rpoB	Variant	168	7	98	88
	Nonvariant	3	52		
embB	Variant	114	4	99	97
	Nonvariant	1	111		
rpsL	Variant	80	6	99	96
	Nonvariant	1	143		
rrs-S	Variant	19	2	100	99
	Nonvariant	0	209		
rrs-A	Variant	8	9	89	96
	Nonvariant	1	212		
eis	Variant	6	1	100	100
	Nonvariant	0	223		
gyrA	Variant	28	8	90	96
	Nonvariant	3	191[a]		
gyrB	Variant	4	5	67	98
	Nonvariant	2	219		
pncA	Variant	81[b]	29	85	79
	Nonvariant	14[c]	106[d]		

[a] One hundred seventy-seven of 191 showed the transversion AGC→ACC (Ser95Thr), a common polymorphism not associated with drug resistance.
[b] Four of 81 contained Ser65Ser along with mutations in other positions.
[c] Two of 14 were transversions.
[d] Sixteen of 106 consisted of a silent mutation (TCC→TCT; Ser65Ser).

M. tuberculosis culture and, thus, would likely not work well in clinical specimens or mixed TB/nontuberculous mycobacterial samples. Additionally, the assay performance appeared suboptimal compared to Sanger sequencing for *pncA*/pyrazinamide (PZA) (accuracy for phenotypic PZA resistance, 82% versus 92%, respectively). Pyrazinamide resistance is an important consideration in the management of MDR-TB, particularly in the face of new TB drugs where pyrazinamide yields synergy (23). This suboptimal performance was largely a function of the microliter format. We previously developed an HRM assay for PZA, using 7 overlapping amplicons in a 20-μl volume on the Rotorgene platform, that yielded a 94% concordance versus Sanger sequencing results (including on many of these isolates) (15), and even 5 μl in a 384-well plate format improved the sensitivity (data not shown). The performance of TAC-HRM was also poor against the phenotypic results for ethambutol, as was that of Sanger sequencing. The major discrepancies were mutations at codons 306 and 406 that were found in susceptible isolates. Such discordance has been reported previously and has brought into question the association with resistance of codon 306 (24–26); however, allelic exchange experiments do demonstrate that codons 306 and 406 can confer resistance (27–29). Such discordance implicates the phenotypic testing for ethambutol as problematic (30, 31). The concordance between the results of *rpoB* and rifampin drug susceptibility testing was slightly lower than expected (88%); however, this was similar to that of sequencing and may reflect some comparisons to a phenotypic standard on Lowenstein-Jensen (L-J) medium. Of the 16 TAC-HRM variant samples that were rifampin susceptible, 1 was a silent mutation, as might be expected, 5 were Leu533Pro, which has been associated with discordant susceptibility results previously (32), and 3 had one of the well-known resistance mutations Ser531Leu and Asp516Val.

Taken together, this TAC-HRM assay yields a highly accurate TB drug susceptibility result versus either sequencing or culture-based methodologies for the most common drugs used to treat

TABLE 2 Correlation of sequencing and TAC-HRM results with phenotypic drug susceptibility test results

Drug	Gene target (no. of isolates tested[a])	Resistance-associated mutation found or not found by sequencing	No. with indicated DST result[f]		% accuracy	TAC-HRM result	No. with indicated DST result		% accuracy
			R	S			R	S	
INH	*inhA* or *katG* (227)	Found	174	0	95	Variant	171	1	93
		Not found	12	41		Nonvariant	15	40	
RIF	*rpoB* (219)	Found	153	11	91	Variant	151	16	88
		Not found	8	47		Nonvariant	10	42	
EMB	*embB* (203)	Found	62	35	74	Variant	60	36	72
		Not found	18[b]	88[b]		Nonvariant	20	87	
STR	*rpsL* or *rrs*-S (190)	Found	81	10	87	Variant	83	11	88
		Not found	14	85		Nonvariant	12	84	
AMK or KAN	*rrs*-A or *eis* (221)	Found	8	8	95	Variant	9	10	94
		Not found	4	201		Nonvariant	3	199	
OFX or MXF	*gyrA* or *gyrB* (220)	Found	31	3	95	Variant	29	10	91
		Not found	9	177[c]		Nonvariant	11	170[c]	
PZA	*pncA* (113)	Found	49	2	92	Variant	45	9	82
		Not found	7[d]	55[e]		Nonvariant	11[d]	48[e]	

[a] The number of isolates is not always 230 because not all isolates were tested with phenotypic assays and isolates with discordant phenotypic results were excluded.
[b] Five of 18 and 22/88 were Glu378Ala, which is a polymorphism not considered associated with drug resistance (10).
[c] One hundred sixty-three of 177 and 156/170 were *gyrA* Ser95Thr, which is a transversion polymorphism not associated with drug resistance.
[d] Two of 7 and 2/11 were a silent mutation (TCC→TCT; Ser65Ser).
[e] Five of 55 and 5/48 were a silent mutation (Ser65Ser).
[f] DST, drug susceptibility test; R, resistant; S, susceptible.

MDR-TB. It carefully interrogates 3,200 bp of *M. tuberculosis* gene territory and can be performed at a modest cost in laboratories with real-time PCR capabilities without postamplification manipulation or risk. The use of such an assay in the clinical setting could improve MDR-TB treatment outcomes and limit the amplification of resistance by identifying the greatest number of active drugs to include in a regimen (2, 3), instead of the current standard of care in most countries where TB is endemic, which is to use a nonindividualized empirical regimen. To this end, it would be sensible to use this device in a tiered setting (33), for example, on MDR-TB cases diagnosed by GeneXpert, where confirmation of MDR-TB and information on other drug susceptibilities is desirable.

MATERIALS AND METHODS

Mycobacterial strains and culture conditions. The mycobacterial strains used in this study included *M. tuberculosis* H37Rv (ATCC 27294) and a total of 230 clinical isolates, including 92 from Bangladesh (International Centre for Diarrheal Diseases and Research, Dhaka), 85 from Thailand (Department of Microbiology, Faculty of Medicine, Siriraj Hospital, Mahidol University, Bangkok), 28 from the Russian Federation (Scientific Center of Family Health and Reproductive Problems, Siberian Branch, Russian Academy of Medical Sciences, Irkutsk), 23 from Tanzania (Kilimanjaro Clinical Research Institute, Moshi), and 2 from the University of Virginia. Most were MDR (72%) based on phenotypic susceptibility testing. *M. tuberculosis* isolates were cultured on Lowenstein-Jensen (L-J) medium at 37°C for 2 to 3 weeks. Cell suspensions were prepared in Middlebrook 7H9 (M7H9) broth supplemented with Middlebrook oleic acid-albumin-dextrose-catalase (OADC) enrichment (Difco, Livonia, MI) and were adjusted to 1 McFarland for the agar proportion and L-J proportion methods and to 0.5 McFarland for MGIT susceptibility testing, TREK Sensititre MYCOTB, and DNA extraction. All work was approved by the University of Virginia Institutional Biosafety Committee and Human Investigation Committees.

Phenotypic drug susceptibility testing. Isolates from Thailand underwent susceptibility testing with the standard agar proportion method for both 1st-line and 2nd-line drugs. Isolates from Tanzania underwent MGIT for 1st-line and TREK Sensititre MYCOTB for both 1st- and 2nd-line drugs. Isolates from Bangladesh were tested using the L-J proportion method for 1st-line and TREK Sensititre MYCOTB for both 1st- and 2nd-line drugs. Twelve isolates from the Russian Federation were tested using the L-J proportion method and TREK Sensititre MYCOTB for both 1st- and 2nd-line drugs, while 16 isolates were tested only with TREK Sensititre MYCOTB. Pyrazinamide susceptibility tests were performed using the MGIT method. All methodologies have been described previously (15, 34, 35).

Sanger sequencing. All 230 TB isolates were sequenced by Sanger sequencing. The amplification and sample preparation for sequencing were described previously (34). The following seven loci were amplified by PCR, using the locus-specific primers of Campbell et al. (10): *inhA* and *katG* (INH), *rpoB* (RIF), *embB* (EMB), *rrs* (KAN, CAP, and AMK), *eis* (KAN), and *gyrA* (OFX and MXF). The *rpsL* (STR), *rrs* (STR), and *gyrB* (OFX and MXF) loci were amplified by the following primers designed in this study: *rpsL*-F, 5′ CCGACAAACAGAACGTGAAA 3′; *rpsL*-R, 5′ ACCAACTGCGATCCGTAGAC 3′; *rrs*S-F, 5′ CTGAGATACGGCCCAGACTC 3′; *rrs*S-R, 5′ TGCATGTCAAACCCAGGTAA 3′; *gyrB*-F, 5′ CGTAAGGCACGAGAGTTGGT 3′; and *gyrB*-R, 5′ GTTGTGCCAAAAACACATGC 3′.

Primer and probe design. The TaqMan array card (TAC) included 27 primer pairs and 40 specific probes, of which 38 specific probes targeted the most common drug resistance-associated mutations of *inhA*, *katG*, *rpoB*, *embB*, *rpsL*, *rrs*, *eis*, *gyrA*, and *gyrB*. Two probes were specific to the *pncA* His57Asp (CAC→GAC) of *M. bovis* and a common silent mutation, Ser65Ser (TCC→TCT). Nine pairs of overlapping primers covered the upstream region and the entire 561-bp *pncA* open reading frame. The primers and probes were designed using Primer Express 3 (Applied Biosystems, Life Technologies Corporation, Carlsbad, CA) unless a reference is cited (Table S2 in the supplemental material). Additionally, one primer/probe specific to *M. tuberculosis* 16S rRNA was included in the card as a PCR positive control.

High-resolution melt plus TaqMan probe assay development. The optimization of conditions and probe specificity testing were performed in the 384-well format of the ViiA 7 platform (Applied Biosystems, Life Technologies Corporation, Carlsbad, CA). Each primer/probe set (0.05 μl each of forward and reverse primer and 0.02 μl of probe from 50 μM stock) was utilized in singleplex amplifications, with 5 μl of PCR mixture containing 2.5 μl of 2× MeltDoctor HRM master mix (Applied Biosystems, Life Technologies Corporation, Carlsbad, CA), 1.38 μl of nuclease-free water, and 1 μl of genomic DNA. The cycling conditions included an initial denaturation step at 95°C for 10 min, followed by 40 cycles of denaturation at 95°C for 15 s and annealing/extension at 64°C for 1 min. For the high-resolution melt, denaturation occurred at 95°C for 1 min, followed by heteroduplex formation at 50°C for 1 min and then by continuous melting from 70 to 95°C at 0.025°C/s. The reference strain *M. tuberculosis* H37Rv was included in each run as a wild-type control for HRM-based analysis and as a negative control for TaqMan probe analysis, and nuclease-free water was used for a nontemplate control.

High-resolution melt plus TaqMan probe assay on microfluidic card format. The optimized primer/probe assay for each gene target allowed singleplex amplification in the microfluidic card format by loading a 100-μl reaction mixture including 50 μl of 2× MeltDoctor HRM master mix, 1 μl each of forward and reverse primer (50 μM), 0.4 μl of probe from a 50 μM stock, 27.6 μl of nuclease-free water, and 20 μl of genomic DNA into an empty microfluidic card that has 8 ports per card, with one sample per port. This was centrifuged twice at 1,200 rpm for 1 min, and then the card was sealed, the loading ports were excised, and the card was inserted into a ViiA 7 instrument (Life Technologies Corporation, Carlsbad, CA) and run under the same cycling conditions as described above. *M. tuberculosis* H37Rv was included in each run as a wild-type control, and either a mutant sample or a constructed DNA plasmid control was used on every run and served as a positive control for mutations.

Evaluation of HRM plus TaqMan probe array card. The primer and probe oligonucleotides were synthesized and spotted onto the microfluidic card by Applied Biosystems (Life Technologies Corporation, Carlsbad, CA). Twenty microliters of input DNA was mixed with 50 μl of 2× MeltDoctor HRM master mix, 2 μl of 2.5 μM ROX reference dye, and 28 μl of water to a 100-μl final volume. This was loaded into each port of the card, whereby each card included six clinical samples, *M. tuberculosis* H37Rv as a wild-type control, and the plasmid containing one mutation of each HRM gene segment as a mutant control for HRM.

TAC-HRM analysis. Since our assay combined HRM and a TaqMan probe in the same reaction, HRM was analyzed first. Melt curve data were analyzed and normalized using the HRM software module for the ViiA 7 system on the basis of the differences in the shapes and temperature shifts of the melt curves of the sample and the *M. tuberculosis* H37Rv wild-type control. The HRM curves were analyzed by selecting two normalization regions, one occurring prior to the melt of the amplicon and one following complete separation of the two strands. The results for each sample were compared to the results for the wild-type control and automatically categorized as wild-type or variant by the software. Each well yielded two amplification plots, one on the MeltDoctor channel (SYTO9) and the other on the fluorophore (VIC/HEX/NED) channel. Then, the parameters were reset for probe-based real-time PCR analysis.

Statistical analysis. Means or medians were compared using the *t* test or Mann-Whitney test. Receiver operating characteristic (ROC) analysis was performed with PASW Statistics software to define a cutoff for categorizing variants by HRM.

SUPPLEMENTAL MATERIAL

Supplemental material for this article may be found at http://mbio.asm.org/lookup/suppl/doi:10.1128/mBio.02273-14/-/DCSupplemental.

Figure S1, TIF file, 1.7 MB.
Figure S2, TIF file, 0.8 MB.
Figure S3, TIF file, 1.8 MB.
Figure S4, TIF file, 0.9 MB.
Table S1, DOCX file, 0.03 MB.
Table S2, DOCX file, 0.1 MB.

ACKNOWLEDGMENTS

This work was supported by NIH grants R01 AI093358 and K24 AI102972 (to E.H.) and Russian Foundation for Basic Research grant 13-04-91445 RFBR-NIH.

REFERENCES

1. **World Health Organization.** 2010, Global tuberculosis control. WHO report 2010. World Health Organization, Geneva, Switzerland.
2. **Ahuja SD, Ashkin D, Avendano M, Banerjee R, Bauer M, Bayona JN, Becerra MC, Benedetti A, Burgos M, Centis R, Chan ED, Chiang CY, Cox H, D'Ambrosio L, DeRiemer K, Dung NH, Enarson D, Falzon D, Flanagan K, Flood J, Garcia-Garcia ML, Gandhi N, Granich RM, Hollm-Delgado MG, Holtz TH, Iseman MD, Jarlsberg LG, Keshavjee S, Kim HR, Koh WJ, Lancaster J, Lange C, de Lange WC, Leimane V, Leung CC, Li J, Menzies D, Migliori GB, Mishustin SP, Mitnick CD, Narita M, O'Riordan P, Pai M, Palmero D, Park SK, Pasvol G, Pena J, Perez-Guzman C, Quelapio MI, Ponce-de-Leon A.** 2012. Multidrug resistant pulmonary tuberculosis treatment regimens and patient outcomes: an individual patient data meta-analysis of 9,153 patients. PLoS Med **9:**e1001300. http://dx.doi.org/10.1371/journal.pmed.1001300.
3. **Bastos ML, Hussain H, Weyer K, Garcia-Garcia L, Leimane V, Leung CC, Narita M, Pena JM, Ponce-de-Leon A, Seung KJ, Shean K, Sifuentes-Osornio J, Van der Walt M, Van der Werf TS, Yew WW, Menzies D, Collaborative Group for Meta-analysis of Individual Patient Data in MDR-TB.** 2014. Treatment outcomes of patients with multidrug-resistant and extensively drug-resistant tuberculosis according to drug susceptibility testing to first- and second-line drugs: an individual patient data meta-analysis. Clin Infect Dis **59:**1364–1374. http://dx.doi.org/10.1093/cid/ciu619.
4. **Cegielski JP, Dalton T, Yagui M, Wattanaamornkiet W, Volchenkov GV, Via LE, Van Der Walt M, Tupasi T, Smith SE, Odendaal R, Leimane V, Kvasnovsky C, Kuznetsova T, Kurbatova E, Kummik T, Kuksa L, Kliiman K, Kiryanova EV, Kim H, Kim CK, Kazennyy BY, Jou R, Huang WL, Ershova J, Erokhin VV, Diem L, Contreras C, Cho SN, Chernousova LN, Chen MP, Caoili JC, Bayona J, Akksilp S.** 2014. Extensive drug resistance acquired during treatment of multidrug-resistant tuberculosis. Clin Infect Dis **59:**1049–1063. http://dx.doi.org/10.1093/cid/ciu572.
5. **Giannoni F, Iona E, Sementilli F, Brunori L, Pardini M, Migliori GB, Orefici G, Fattorini L.** 2005. Evaluation of a new line probe assay for rapid identification of gyrA mutations in Mycobacterium tuberculosis. Antimicrob Agents Chemother **49:**2928–2933. http://dx.doi.org/10.1128/AAC.49.7.2928-2933.2005.
6. **Huang WL, Chen HY, Kuo YM, Jou R.** 2009. Performance assessment of the GenoType MTBDRplus test and DNA sequencing in detection of multidrug-resistant Mycobacterium tuberculosis. J Clin Microbiol **47:**2520–2524. http://dx.doi.org/10.1128/JCM.02499-08.
7. **Mäkinen J, Marttila HJ, Marjamäki M, Viljanen MK, Soini H.** 2006. Comparison of two commercially available DNA line probe assays for detection of multidrug-resistant Mycobacterium tuberculosis. J Clin Microbiol **44:**350–352. http://dx.doi.org/10.1128/JCM.44.2.350-352.2006.
8. **Blakemore R, Story E, Helb D, Kop J, Banada P, Owens MR, Chakravorty S, Jones M, Alland D.** 2010. Evaluation of the analytical performance of the Xpert MTB/RIF assay. J Clin Microbiol **48:**2495–2501. http://dx.doi.org/10.1128/JCM.00128-10.
9. **Malik S, Willby M, Sikes D, Tsodikov OV, Posey JE.** 2012. New insights into fluoroquinolone resistance in Mycobacterium tuberculosis: functional genetic analysis of gyrA and gyrB mutations. PLoS One **7:**e39754. http://dx.doi.org/10.1371/journal.pone.0039754.
10. **Campbell PJ, Morlock GP, Sikes RD, Dalton TL, Metchock B, Starks AM, Hooks DP, Cowan LS, Plikaytis BB, Posey JE.** 2011. Molecular detection of mutations associated with first- and second-line drug resistance compared with conventional drug susceptibility testing of Mycobacterium tuberculosis. Antimicrob Agents Chemother **55:**2032–2041. http://dx.doi.org/10.1128/AAC.01550-10.
11. **Pholwat S, Stroup S, Foongladda S, Houpt E.** 2013. Digital PCR to detect and quantify heteroresistance in drug resistant Mycobacterium tuberculosis. PLoS One **8:**e57238. http://dx.doi.org/10.1371/journal.pone.0057238.
12. **Kodani M, Yang G, Conklin LM, Travis TC, Whitney CG, Anderson LJ, Schrag SJ, Taylor TH, Jr, Beall BW, Breiman RF, Feikin DR, Njenga MK, Mayer LW, Oberste MS, Tondella ML, Winchell JM, Lindstrom SL, Erdman DD, Fields BS.** 2011. Application of TaqMan low-density arrays for simultaneous detection of multiple respiratory pathogens. J Clin Microbiol **49:**2175–2182. http://dx.doi.org/10.1128/JCM.02270-10.
13. **Liu J, Gratz J, Amour C, Kibiki G, Becker S, Janaki L, Verweij JJ, Taniuchi M, Sobuz SU, Haque R, Haverstick DM, Houpt ER.** 2013. A laboratory-developed TaqMan array card for simultaneous detection of 19 enteropathogens. J Clin Microbiol **51:**472–480. http://dx.doi.org/10.1128/JCM.02658-12.
14. **Choi GE, Lee SM, Yi J, Hwang SH, Kim HH, Lee EY, Cho EH, Kim JH, Kim HJ, Chang CL.** 2010. High-resolution melting curve analysis for rapid detection of rifampin and isoniazid resistance in Mycobacterium tuberculosis clinical isolates. J Clin Microbiol **48:**3893–3898. http://dx.doi.org/10.1128/JCM.00396-10.
15. **Pholwat S, Stroup S, Gratz J, Trangan V, Foongladda S, Kumburu H, Juma SP, Kibiki G, Houpt E.** 2014. Pyrazinamide susceptibility testing of Mycobacterium tuberculosis by high resolution melt analysis. Tuberculosis (Edinb) **94:**20–25.
16. **Ramirez MV, Cowart KC, Campbell PJ, Morlock GP, Sikes D, Winchell JM, Posey JE.** 2010. Rapid detection of multidrug-resistant Mycobacterium tuberculosis by use of real-time PCR and high-resolution melt analysis. J Clin Microbiol **48:**4003–4009. http://dx.doi.org/10.1128/JCM.00812-10.
17. **Chen X, Kong F, Wang Q, Li C, Zhang J, Gilbert GL.** 2011. Rapid detection of isoniazid, rifampin, and ofloxacin resistance in Mycobacterium tuberculosis clinical isolates using high-resolution melting analysis. J Clin Microbiol **49:**3450–3457. http://dx.doi.org/10.1128/JCM.01068-11.
18. **Lee AS, Ong DC, Wong JC, Siu GK, Yam WC.** 2012. High-resolution melting analysis for the rapid detection of fluoroquinolone and streptomycin resistance in Mycobacterium tuberculosis. PLoS One **7:**e31934. http://dx.doi.org/10.1371/journal.pone.0031934.
19. **Wang F, Shen H, Guan M, Wang Y, Feng Y, Weng X, Wang H, Zhang W.** 2011. High-resolution melting facilitates mutation screening of rpsL gene associated with streptomycin resistance in Mycobacterium tuberculosis. Microbiol Res **166:**121–128. http://dx.doi.org/10.1016/j.micres.2010.02.001.
20. **Rodwell TC, Valafar F, Douglas J, Qian L, Garfein RS, Chawla A, Torres J, Zadorozhny V, Kim MS, Hoshide M, Catanzaro D, Jackson L, Lin G, Desmond E, Rodrigues C, Eisenach K, Victor TC, Ismail N, Crudu V, Gler MT, Catanzaro A.** 2014. Predicting extensively drug-resistant Mycobacterium tuberculosis phenotypes with genetic mutations. J Clin Microbiol **52:**781–789. http://dx.doi.org/10.1128/JCM.02701-13.
21. **Sandgren A, Strong M, Muthukrishnan P, Weiner BK, Church GM, Murray MB.** 2009. Tuberculosis drug resistance mutation database. PLoS Med **6:**e2. http://dx.doi.org/10.1371/journal.pmed.1000002.
22. **Liu J, Kabir F, Manneh J, Lertsethtakarn P, Begum S, Gratz J, Becker SM, Operario DJ, Taniuchi M, Janaki L, Platts-Mills JA, Haverstick DM, Kabir M, Sobuz SU, Nakjarung K, Sakpaisal P, Silapong S, Bodhidatta L, Qureshi S, Kalam A, Saidi Q, Swai N, Mujaga B, Maro A, Kwambana B, Dione M, Antonio M, Kibiki G, Mason CJ, Haque R, Iqbal N, Zaidi AK, Houpt ER.** 2014. Development and assessment of molecular diagnostic tests for 15 enteropathogens causing childhood diarrhoea: a multicentre study. Lancet Infect Dis **14:**716–724. http://dx.doi.org/10.1016/S1473-3099(14)70808-4.
23. **Tasneen R, Li SY, Peloquin CA, Taylor D, Williams KN, Andries K, Mdluli KE, Nuermberger EL.** 2011. Sterilizing activity of novel TMC207- and PA-824-containing regimens in a murine model of tuberculosis. Antimicrob Agents Chemother **55:**5485–5492. http://dx.doi.org/10.1128/AAC.05293-11.
24. **Shi D, Li L, Zhao Y, Jia Q, Li H, Coulter C, Jin Q, Zhu G.** 2011. Characteristics of embB mutations in multidrug-resistant Mycobacterium tuberculosis isolates in Henan, China. J Antimicrob Chemother **66:**2240–2247. http://dx.doi.org/10.1093/jac/dkr284.
25. **Bakuła Z, Napiórkowska A, Bielecki J, Augustynowicz-Kopeć E, Zwolska Z, Jagielski T.** 2013. Mutations in the embB gene and their association with ethambutol resistance in multidrug-resistant Mycobacterium tuber-

culosis clinical isolates from Poland. Biomed Res Int **2013:**167954. http://dx.doi.org/10.1155/2013/167954.

26. **Shi R, Zhang J, Otomo K, Zhang G, Sugawara I.** 2007. Lack of correlation between embB mutation and ethambutol MIC in Mycobacterium tuberculosis clinical isolates from China. Antimicrob Agents Chemother **51:**4515–4517. http://dx.doi.org/10.1128/AAC.00416-07.
27. **Safi H, Fleischmann RD, Peterson SN, Jones MB, Jarrahi B, Alland D.** 2010. Allelic exchange and mutant selection demonstrate that common clinical embCAB gene mutations only modestly increase resistance to ethambutol in Mycobacterium tuberculosis. Antimicrob Agents Chemother **54:**103–108. http://dx.doi.org/10.1128/AAC.01288-09.
28. **Safi H, Sayers B, Hazbón MH, Alland D.** 2008. Transfer of embB codon 306 mutations into clinical Mycobacterium tuberculosis strains alters susceptibility to ethambutol, isoniazid, and rifampin. Antimicrob Agents Chemother **52:**2027–2034. http://dx.doi.org/10.1128/AAC.01486-07.
29. **Starks AM, Gumusboga A, Plikaytis BB, Shinnick TM, Posey JE.** 2009. Mutations at embB codon 306 are an important molecular indicator of ethambutol resistance in Mycobacterium tuberculosis. Antimicrob Agents Chemother **53:**1061–1066. http://dx.doi.org/10.1128/AAC.01357-08.
30. **Krüüner A, Yates MD, Drobniewski FA.** 2006. Evaluation of MGIT 960-based antimicrobial testing and determination of critical concentrations of first- and second-line antimicrobial drugs with drug-resistant clinical strains of Mycobacterium tuberculosis. J Clin Microbiol **44:**811–818. http://dx.doi.org/10.1128/JCM.44.3.811-818.2006.
31. **Angra PK, Taylor TH, Iademarco MF, Metchock B, Astles JR, Ridderhof JC.** 2012. Performance of tuberculosis drug susceptibility testing in U.S. laboratories from 1994 to 2008. J Clin Microbiol **50:**1233–1239. http://dx.doi.org/10.1128/JCM.06479-11.
32. **Van Deun A, Barrera L, Bastian I, Fattorini L, Hoffmann H, Kam KM, Rigouts L, Rüsch-Gerdes S, Wright A.** 2009. Mycobacterium tuberculosis strains with highly discordant rifampin susceptibility test results. J Clin Microbiol **47:**3501–3506. http://dx.doi.org/10.1128/JCM.01209-09.
33. **Salfinger M, Pfyffer GE.** 1994. The new diagnostic mycobacteriology laboratory. Eur J Clin Microbiol Infect Dis **13:**961–979. http://dx.doi.org/10.1007/BF02111498.
34. **Pholwat S, Ehdaie B, Foongladda S, Kelly K, Houpt E.** 2012. Real-time PCR using mycobacteriophage DNA for rapid phenotypic drug susceptibility results for Mycobacterium tuberculosis. J Clin Microbiol **50:**754–761. http://dx.doi.org/10.1128/JCM.01315-11.
35. **Banu S, Rahman SM, Khan MS, Ferdous SS, Ahmed S, Gratz J, Stroup S, Pholwat S, Heysell SK, Houpt ER.** 2014. Discordance across several methods for drug susceptibility testing of drug-resistant Mycobacterium tuberculosis isolates in a single laboratory. J Clin Microbiol **52:**156–163. http://dx.doi.org/10.1128/JCM.02378-13.